Entropy Production in a Chaotic Chemical System

Kristian Lindgren and Bengt Å. G. Månsson
Physical Resource Theory Group, Chalmers University of Technology
and University of Göteborg, Sweden

Z. Naturforsch. **41 a,** 1111–1117 (1986); received April 30, 1986

The average rate of entropy production in a homogenous chemical system is investigated in oscillating periodic and chaotic modes as well as in coexisting stationary states. The simulations are based on an abstract model of a chemical reaction system with three freely varying concentrations. Five concentrations are assumed to be kept constant by suitable flows across the boundary. A fixed concentration is used as a control parameter. Second order mass action kinetics with reverse reaction is used. An unexpected result is that periodic modes in some windows in the chaotic interval have higher average rate of entropy production than the surrounding chaotic modes. A chaotic mode coexists with a stable stationary state with smaller entropy production. A unique (unstable) stationary state produces more entropy than the corresponding oscillating mode.

1. Introduction

During the last two decades there has been an explosive development of both experimental and theoretical research on chemical systems evolving far from equilibrium. Exotic behaviour such as multistability, oscillations, spatial self-organization and chaotic evolution has been studied theoretically and found experimentally in numerous chemical systems [1–4]. The interest has not only focused on these exotic phenomena as such, it has also been turned towards more general issues, such as the thermodynamics of nonlinear, far-from-equilibrium systems, and the implications for biological systems [5, 6].

The present paper studies the rate of dissipative losses, i.e., the rate of entropy production, due to chemical reactions in autonomous chemical oscillators. (For a recent study of the dissipative in non-autonomous chemical oscillators, see Richter [7].) In [8], the behaviour of the rate of entropy production was investigated in the neighbourhood of a Hopf bifurcation and for the associated periodic trajectories. Here, a similar investigation is made for a typical oscillating system with period-doubling bifurcations and chaos. The central issue is the average rate of entropy production in different oscillating modes. This is one relevant measure of the efficiency of oscillatory behaviour, with possible implications for, e.g., metabolic processes.

Willamowski and Rössler [9] have proposed an abstract realistic chemical reaction system (based on at most second order elementary reactions) which both satisfies the requirements of thermodynamics and exhibits chaotic behaviour. Since our numerical simulations are based on this system, a thorough investigation was made of its properties. Thus, further numerical evidence that their system actually is chaotic is provided, as well as some new features of its stationary and dynamical behaviour.

Since the aim is to investigate some typical features of general open chemical systems, a number of conventional simplifying assumptions are made. The system is assumed to be *isothermal* and *homogenous*. (For an open chemical system with oscillating concentrations, the assumption implies that the mixing processes (diffusion and stirring) are fast compared to the chemical reactions.) The *local equilibrium approximation* is assumed to be valid. The reaction laws follows the simplest form of the *law of mass action* in ideal gases.

Reprint requests to Bengt Månsson, Physical Resource Theory Group, Chalmers University of Technology, S-412 96 Göteborg, Sweden.

2. Average Entropy Production Rate

Let the vector $\boldsymbol{x}(t)$ denote the state of a general system obeying the equations of motion

$$\dot{\boldsymbol{x}} = \boldsymbol{f}(\boldsymbol{x}; \alpha) , \tag{1}$$

0340-4811 / 86 / 0900-1111 $ 01.30/0. – Please order a reprint rather than making your own copy.

where α is a scalar control parameter characterizing f. Assume that the system (1) has a periodic trajectory x^0 with period τ for a certain parameter value α^0, i.e., for $x(t) \in x^0$,

$$x(t) = x(t+\tau) . \tag{2}$$

Then, denoting the entropy production rate (defined in Sect. 4) by $\sigma(x(t))$, the average entropy production rate is defined by

$$\bar{\sigma}(\alpha^0) = \tau^{-1} \int_0^\tau \sigma(x(t))\, dt , \tag{3}$$

where $x(t) \in x^0$. As indicated, it can be treated as a function of α^0. Equation (3) is the basic expression of this paper.

In [8], the central issue was the difference between the rate of entropy production on a stable periodic trajectory and in a corresponding unstable stationary state. A similar variable can be introduced in the present framework for parameter values α such that there exist both stable and unstable closed trajectories. Then, for each pair of trajectories, an entropy production rate difference, Δ, can be defined by

$$\Delta(\alpha) = \bar{\sigma}(\alpha) - \bar{\sigma}_u(\alpha) , \tag{4}$$

where the subscript u indicates that $\bar{\sigma}_u$ is calculated on an unstable trajectory. Although at least one such unstable trajectory always exists in a neighbourhood of a period-doubling bifurcation, it may be difficult to find in general. One reason is that although the trajectory is unstable, i.e., neighbouring trajectories diverge, this may be only in some directions, while trajectories in other directions are attracted. A simple reversal of the equations of motion will then only reverse the roles of these directions, leaving the trajectory unstable. (Numerical methods for finding an unstable trajectory are described in [10].) Note that the periods of the trajectories in (4) may differ, even modulo an integer factor. Generally, the relationship between orbital stability and entropy production cannot be given such a simple formulation as the corresponding theorem in linear thermodynamics [5].

Similarly, for any two closed trajectories characterized by α' and α'', an entropy production rate difference, $\Xi(\alpha', \alpha'')$, can be generally defined by

$$\Xi(\alpha'', \alpha') = \bar{\sigma}(\alpha'') - \bar{\sigma}(\alpha') . \tag{5}$$

Note that in many cases reaction rates vary very little with small displacements in state space. Therefore trajectories that are everywhere close in state space have roughly equal periods, modulo an integer factor.

Assume that $x'(t)$, characterized by α', has period τ and that the period of $x^*(t)$, characterized by α^*, approaches 2τ as $\alpha^* \to \alpha'$,

$$x^*(t) = x^*(t + 2\tau) , \tag{6}$$

i.e., α' is a period-doubling bifurcation value. Then a vector δ can be defined by

$$\delta(t) = x^*(t) - x'(t) . \tag{7}$$

If

$$|\delta(t)| = |x^*(t) - x'(t)| \ll 1 , \tag{8}$$

i.e., the closed trajectories lie close to each other in state space and the phase differences are small everywhere, then Ξ can be expanded in terms of δ,

$$\Xi(\alpha^*, \alpha') \tag{9}$$

$$= (2\tau)^{-1} \int_0^{2\tau} \{D_1(x'(t)) \cdot \delta(t) + \delta(t) \cdot D_2(x'(t)) \cdot \delta(t)/2 + \ldots\}\, dt , \tag{9}$$

where

$$D_1 = \nabla\sigma(x) \tag{10}$$

and

$$D_2 = \nabla\nabla\sigma(x) . \tag{11}$$

A similar expansion can be made of $\Delta(\alpha^*)$ if the period times of the stable and unstable trajectories are simply related. As argued above this is likely to be the case if they lie close in state space. Using the methodology in [11] (Sect. 8.7) it is at least in principle possible to find $\delta(t)$, knowing α' and $x'(t)$. It may then be possible to save computation time by using (9) instead of (4) or (5).

3. The Model

To illustrate the behaviour of the rate of entropy production and the entropy production rate difference, the abstract system of chemical reactions formulated by Willamowski and Rössler [9] will be used. The model is given by the reaction scheme

$$A + X \rightleftharpoons 2X , \tag{12a}$$

$$X + Y \rightleftharpoons 2Y , \tag{12b}$$

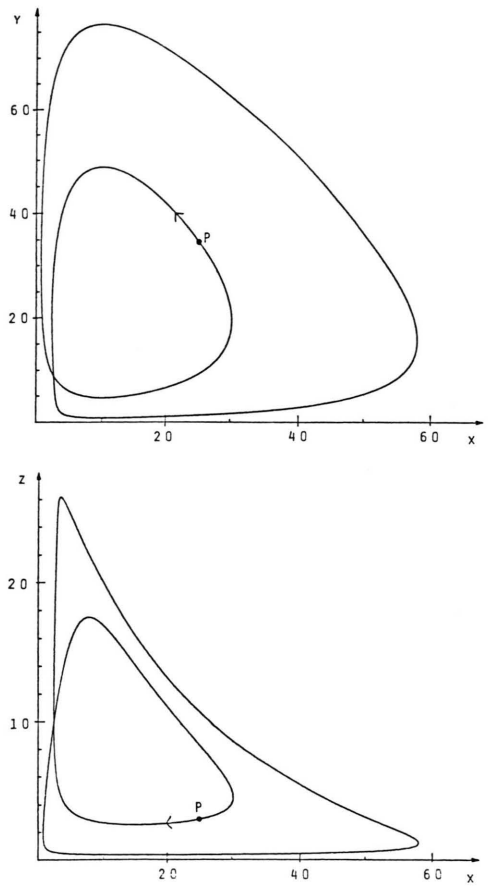

Fig. 1. Projections onto the $x-y$ and $x-z$ planes of the double loop trajectory for $a = 31.5$. The point P marks the same point in both projections and the arrow the direction of movement.

Table 1. Reaction rates J_i and affinities A_i.

i	J_i	$\exp(A_i/RT)$	Reaction
1	$k_1 ax - k_{-1}x^2$	$k_1 a/k_{-1}x$	(12a)
2	$k_2 xy - k_{-2}y^2$	$k_2 x/k_{-2}y$	(12b)
3	$k_3 bz - k_{-3}z^2$	$k_3 b/k_{-3}z$	(12c)
4	$k_4 cy - k_{-4}d$	$k_4 cy/k_{-4}d$	(12d)
5	$k_5 xz - k_{-5}e$	$k_5 xz/k_{-5}e$	(12e)

$$B + Z \rightleftharpoons 2Z\,, \tag{12c}$$
$$C + Y \rightleftharpoons D\,, \tag{12d}$$
$$X + Z \rightleftharpoons E\,, \tag{12e}$$

Note that it contains no third order reaction, but on the other hand it has no less than three auto-catalytic reactions. Also all reverse reactions are allowed.

The concentrations of X, Y, and Z are allowed to vary, all others are assumed to be kept constant by compensating flows across the boundary. However, X, Y, and Z cannot pass the boundary. Denoting the concentrations with corresponding lower-case letters and forward and reverse reaction rate constants by k_i and k_{-i} $(i = 1, \ldots, 5)$ respectively, we get the individual reaction rates J_i as given in Table 1.

The rate expressions are

$$\dot{x} = J_1 - J_2 - J_5\,, \tag{13a}$$
$$\dot{y} = J_2 - J_4\,, \tag{13b}$$
$$\dot{z} = J_3 - J_5\,. \tag{13c}$$

The control parameter is the concentration of A. For the other parameters we use the values of [9], i.e.,

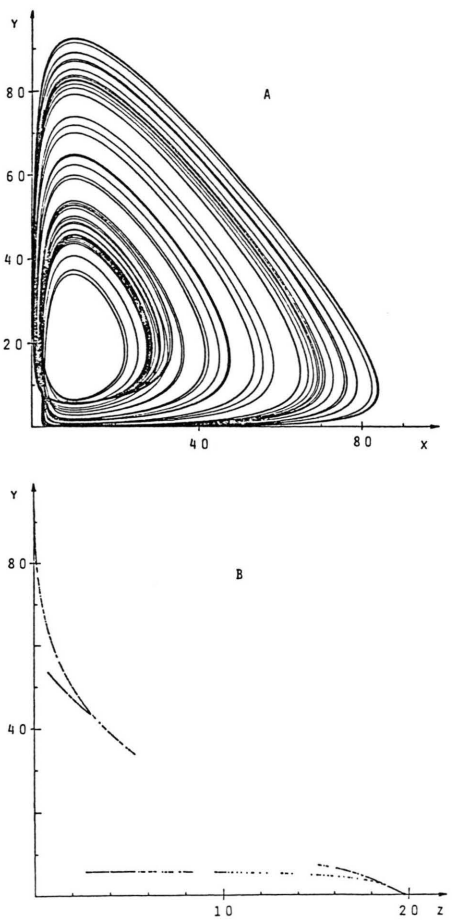

Fig. 2. A) Projection onto the $x-y$ plane of approximately fifty 'loops' of a chaotic trajectory for $a = 30.0$. B) Poincaré map of a chaotic trajectory for $a = 30.0$ (1024 intersections with the plane $x = 10$). The upper "sheet" represents intersections with increasing x, the lower with decreasing x.

$k_1 = k_2 = k_3 = k_4 = k_{-4} = k_5 = k_{-5} = 1$, $k_{-1} = 0.25$, $k_{-2} = 0.001$, $k_{-3} = 0.5$, $b = 16.5$, $c = 10.0$, and $d = e = 0.01$. Figure 1 shows a typical periodic trajectory and Fig. 2 a typical chaotic trajectory.

4. Entropy Production in the Model

The rate of entropy production due to the chemical reactions is given by the sum of products of the individual reaction rates, J_i, and the corresponding affinities, A_i,

$$\sigma = (T^{-1}) \sum_i J_i A_i . \tag{14}$$

The affinitiy of reaction i is defined by

$$A_i = - \sum_j v_{ij} \mu_j , \tag{15}$$

where v_{ij} is the stoichiometric coefficient of j ($j = x$, y, z) in reaction i, and μ_j is the chemical potential of j. We use the expression for the chemical potential in a mixture of ideal gases or in a dilute solution,

$$\mu_j = \mu_j^0 + RT \ln x_j , \tag{16}$$

where μ_j^0 is the standard state chemical potential and x_j denotes the molar fraction. (We have used $R = 1$ in the calculations.) Using the fact that affinities and reaction rates are zero in the thermostatic equilibrium, we get the affinity expressions in Table 1. The terms in the sum in (14) are clearly all non-negative, and zero only if the individual reaction rates are zero.

5. Stationary States and Stability

The system can have multiple stationary states for certain control parameter values, i.e., there can be several solution to the equations

$$\dot{x} = \dot{y} = \dot{z} = 0 . \tag{17}$$

The character and local stability properties of the stationary states are evaluated in the usual manner via the eigenvalues of the Jacobian matrix of $\boldsymbol{f}$ (given below) evaluated at the stationary state [11]. Leaving out some inessential fine-structure, there are the following stationary state characteristics in the interval of parameter values from 0 to 100:

$0 < a < 15.7$	One stable node
$15.8 < a < 17.9$	One stable node, two unstable nodes
$18.0 < a < 32.7$	One stable node, one unstable node, one unstable focus
$32.8 < a < 53$	One unstable focus
$54 < a < 100$	One stable focus

Here, "focus" means that $\mathrm{Im}(\Lambda)$ is non-zero for two complex-conjugate eigenvalues Λ, and "node" indicates that $\mathrm{Im}(\Lambda) = 0$ for all Λ. A stationary state is stable if $\mathrm{Re}(\Lambda) < 0$, unstable if $\mathrm{Re}(\Lambda) > 0$.

6. Dynamical Behaviour

To visualize the trajectory $\boldsymbol{x}(t)$, a Poincaré map (see for example [12]) was constructed by defining a plane (here the plane $x = 10$) in state space and plotting the points of intersection of the trajectory with this plane. A periodic trajectory is represented by at most a few points on such a plane. These points will trace out curves on the plane as the control parameter is varied. Figure 3 shows how the projection of the set of points (corresponding to only one direction of passage through the plane) onto the line $x = 10$, $z = 0$, i.e., the y values of the intersections, varies with the control parameter. Several period doublings and a window in the chaotic interval with a periodic trajectory are clearly visible. For

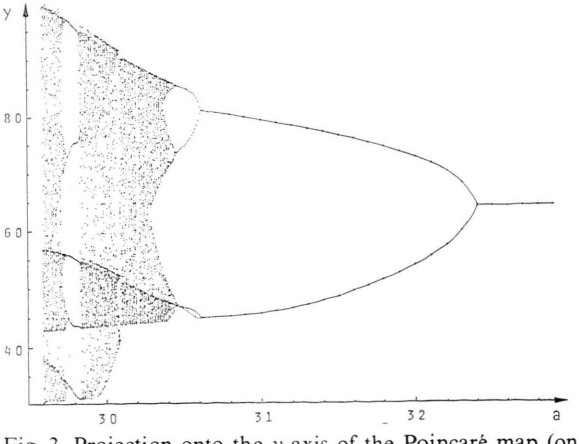

Fig. 3. Projection onto the y-axis of the Poincaré map (on the plane $x = 10$, and intersections in one direction only) over the interval $29.6 \leqq a \leqq 33.0$, where there are several period doublings and intervals with chaos.

chaotic modes the points are sprinkled over intervals on the y axis, cf. the typical trajectory in Figure 2.

The *Lyapounov exponents* [13] measure the average rate of divergence of trajectories. They can be used to define chaos [12, 14–18]. If all Lyapounov exponents are negative the system approaches a stable stationary state. If one exponent vanishes while the other two (presuming a three-dimensional system) are negative $\boldsymbol{x}(t)$ tends asymptotically to a periodic limit cycle. If two exponents vanish and the third one is negative, $\boldsymbol{x}(t)$ either lies on a (stable) torus or is a trajectory corresponding to a period-doubling bifurcation. If there is one positive, one vanishing, and one negative Lyapounov exponent $\boldsymbol{x}(t)$ lies on a *chaotic attractor.*

The Lyapounov exponents were calculated using the method of Frøyland [14] and Frøyland and Alfsen [15] (see also [16]). For a three-dimensional system one uses matrices $M^{(k)}(t)$ $(k = 0, 1, 2, 3)$ defined through

$$M^{(0)}(t) \equiv 1\,, \tag{18}$$

$$M^{(1)}(t) = J\,, \tag{19}$$

$$M^{(2)}(t) = I \cdot \mathrm{Tr}(J) - J^T\,, \tag{20}$$

$$M^{(3)}(t) = \mathrm{Tr}(J)\,, \tag{21}$$

where I is the unit matrix and $J(\boldsymbol{x}(t))$ the Jacobian matrix of $\boldsymbol{f}$ (superscript T stands for transpose). The three Lyapounov exponents are given by

$$\lambda_k = \lim_{t\to\infty} \{t^{-1} \ln[|S^{(k)}(t)/S^{(k-1)}(t)|]\}\,, \quad k = 1, 2, 3\,, \tag{22}$$

where

$$S^{(k)}(t) = \mathrm{Tr}(D^{(k)}(t))\,, \tag{23}$$

and where $D^{(k)}(t)$ is the solution of

$$\dot{D}^{(k)}(t) = M^{(k)}(t) \cdot D^{(k)}(t)\,, \tag{24}$$

integrated along the trajectory $\boldsymbol{x}(t)$, with initial conditions

$$D^{(0)}(0) = D^{(3)}(0) = 1 \quad \text{and} \quad D^{(1)}(0) = D^{(2)}(0) = I\,.$$

We exploited the fact that asymptotically it suffices to consider the time evolution of one of the columns of $D^{(k)}$ to save computation time. For the model (13) and our parameter choices J is given by

$$J = \begin{pmatrix} a - 0.5x - y - z & 0.002y - x & -x \\ y & x - 0.002y - c & 0 \\ -z & 0 & b - x - z \end{pmatrix}. \tag{25}$$

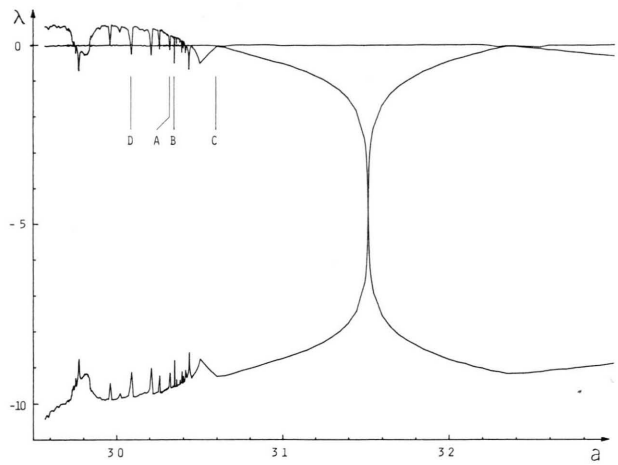

Fig. 4. Lyapounov exponents for $29.6 \leqq a \leqq 33.0$ showing several intervals with positive Lyapounov exponents, i.e. chaos. The plot was constructed by joining points from a simulation, with extra accuracy for $29.70 \leqq a \leqq 29.85$, $30.26 \leqq a \leqq 30.46$ and $31.50 \leqq a \leqq 31.55$. The window around $a = 29.8$ corresponds to a five-loop period doubling sequence (cf. Figure 3). A, B, and D indicate windows in the chaotic interval with periodic trajectories for which the average entropy production rate was calculated, and C is a period doubling, cf. Figure 5.

Figure 4 shows the Lyapounov exponents. Comparison with Fig. 3 shows that two exponents are zero at each period doubling. (The calculations were performed for all three exponents, since the deviation of the vanishing exponent from zero is an indication of the accuracy of the numerical calculations.) There are also several intervals where one exponent is positive, i.e., where chaotic modes exist. A comparison with the analysis of the stationary states shows that there is also a locally stable stationary state for these parameter values. There are thus at least two basins of attraction [16] in state space, one in which trajectories are attracted to the stable stationary state (this basin contains the unstable node), and one where periodic or chaotic motions can occur.

7. Entropy Production – Simulation Results and Discussion

The equations of motion were solved numerically using the Merson variable step-length integration routine. The average rate of entropy production was calculated according to (3) for periodic trajectories. For chaotic trajectories a sampling procedure was

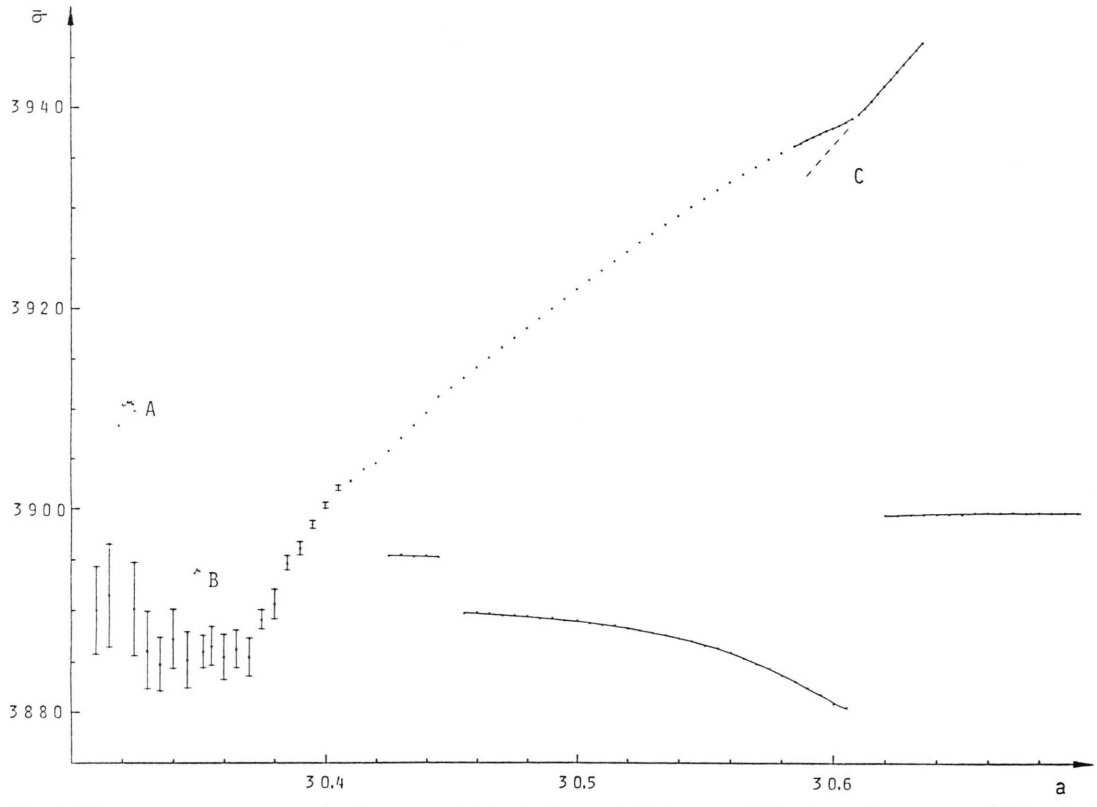

Fig. 5. The average entropy production rate $\bar{\sigma}(a)$ in the interval $30.3 \leqq a \leqq 30.7$, where the system exhibits chaotic as well as periodic behaviour. The dashed curve at C represents a continuation of $\bar{\sigma}(a)$ for the original trajectory at the period doubling. The inserted full-drawn step-like curve in the lower right-hand corner shows the derivative $d\bar{\sigma}/da$. For chaotic modes the mean of the distribution of $\bar{\sigma}(a)$ is shown as the midpoint of a bar two standard deviations long. The dots at A and B represent periodical trajectories from period doubling sequences in windows in the chaotic interval.

utilized, such that the value of (3) was calculated for non-overlapping time-intervals. The length of a time interval (τ in (3)) was determined by following the trajectory (from the zeroth) to the 256th intersection with the Poincaré plane. This gave a distribution of $\bar{\sigma}$ values, and the mean of this distribution is regarded as the average rate of entropy production.

It is natural to ask whether the average entropy production is lower on a periodic or chaotic trajectory than in a stationary state, see Table 2. For $a > 32.8$ the average entropy production on a periodic trajectory is smaller than in the corresponding unique unstable stationary state. However, there is no general rule that the entropy production is smaller in an oscillating mode than it would be if the system stayed in some of the available stationary states. This is clear also from the intervals where there are three stationary states, two of which have lower entropy production than the average on the corresponding limit cycle. In other words, the system has a smaller entropy production in an oscillating mode for some combinations of driving forces, but not for all.

An unexpected feature is the behaviour of the average entropy production in the windows in the chaotic interval where there are periodic trajectories. Figure 5 shows that periodic trajectories in two of these windows (A and B in Fig. 5) correspond to maxima in $\bar{\sigma}(a)$. In other words, in these cases the chaotic modes have smaller entropy production than the neighbouring periodic modes. (This is contrary to the (intuitive) association of orderly behaviour and low entropy production, which is valid in linear thermodynamics [5, 6].) On the other hand, simulations for $a = 30.10$ (D in Fig. 4) and $a = 30.21$ indicate that the difference in $\bar{\sigma}(a)$ between periodic and neighbouring chaotic modes can

Table 2. Rate of entropy production in stationary states and averaged over trajectories. Note that interpolation between values in the table is impossible, especially in the chaotic interval, cf. Figure 5. P = Periodic, C = Chaotic.

a	Stable node	Unstable node	Unstable focus	$\bar{\sigma}$
29.4	1.05	764	4260	–
29.8	1.20	691	4340	3670 P
30.2	1.39	614	4420	3870 C
30.6	1.65	535	4500	3940 C
31.0	2.01	452	4580	4050 P
31.4	2.55	367	4650	4170 P
31.8	3.47	278	4730	4280 P
32.2	5.36	185	4810	4380 P
32.6	12.0	84.9	4890	4470 P
33.0	Nodes merged		4970	4550 P
33.4			5050	4640 P

also be negative (or negligible) for some of the (infinitely many) windows in the chaotic interval.

As shown in Fig. 5, the derivative $d\bar{\sigma}/da$, while remaining positive, changes drastically at each period doubling. There seems to be no discernible rule for determining whether the derivative increases or decreases at a period doubling. The sign of the difference Δ in (4) in the neighbourhood of a period doubling may be positive or negative. In fact, if the average entropy production $\bar{\sigma}_u$ is approximated by an extrapolation (as indicated by the dashed curve marked C in Fig. 5), the curve for $d\bar{\sigma}/da$ shows that both cases occur in the present system.

The results presented here indicate several interesting areas for future research, especially on the theoretical side. There is the classification problem, i.e., whether one can find criteria which identify classes of systems with particular behaviour of the rate of entropy production, especially in windows in chaotic intervals. There is also the question of the behaviour of the functions Δ and Ξ for general classes of systems. Given the fact that a stable stationary state coexists with chaos in the present system, one should analyze the role of fluctuations in such systems, especially the possibility for communication between the different regions in state space. It would also be very interesting to know more about the entropy production in real chemical systems, especially microbiological systems.

We thank Predrag Cvitanović and Karl-Erik Eriksson for their critical reading of the manuscript. This work was supported by the Swedish Natural Science Research Council.

[1] C. Vidal and A. Pacault, eds., Non-Equilibrium Dynamics in Chemical Systems, Springer-Verlag, Berlin 1984.
[2] C. Vidal and A. Pacault, eds., Nonlinear Phenomena in Chemical Dynamics, Springer-Verlag, Berlin 1981.
[3] R. J. Field and M. Burger, eds., Oscillations and Travelling Waves in Chemical Systems, John Wiley, New York 1984.
[4] I. R. Epstein, Complex Dynamical Behavior in "Simple" Chemical Systems, J. Phys. Chem. **88,** 187 (1984).
[5] G. Nicolis and I. Prigogine, Self-organization in Non-equilibrium Systems, John Wiley, New York 1977.
[6] A. R. Peacocke, The Physical Chemistry of Biological Organization, Oxford University Press, Oxford 1983.
[7] P. H. Richter, Physica **10 D,** 353 (1984).
[8] B. Å. G. Månsson, Z. Naturforsch. **40 a,** 877 (1985).
[9] K.-D. Willamowski and O. E. Rössler, Z. Naturforsch. **35 a,** 317 (1980).
[10] M. Kubíček and M. Marek, Computational Methods in Bifurcation Theory and Dissipative Structures, Springer-Verlag, New York 1983.
[11] J. Guckenheimer and P. Holmes, Nonlinear Oscillations, Dynamical Systems and Bifurcations of Vector Fields, Springer-Verlag, New York 1983.
[12] H. Haken, Advanced Synergetics, Springer-Verlag, Berlin 1984.
[13] V. I. Oseledec, Trans. Moscow Math. Soc. **19,** 197 (1968).
[14] J. Frøyland, Physics Letters **97 A,** 8 (1983).
[15] J. Frøyland and K. H. Alfsen, Phys. Rev. **29 A,** 2928 (1984).
[16] J.-P. Eckmann and D. Ruelle, Rev. Mod. Phys. **57** (3), 617 (1985).
[17] R. Shaw, Z. Naturforsch. **36 a,** 80 (1981).
[18] P. Cvitanović, ed., Universality in Chaos, Adam Hilger Ltd, Bristol 1984.